Parallel Helical Domains in DNA Branched Junctions Containing 5′,5′ and 3′,3′ Linkages†

Ruojie Sha,‡ Furong Liu,‡ Michael F. Bruist,§ and Nadrian C. Seeman*,‡

Department of Chemistry, New York University, New York, New York 10003, and Department of Chemistry and Biochemistry, University of the Sciences in Philadelphia, 600 South 43rd St., Philadelphia, Pennsylvania 19104

Received September 30, 1998; Revised Manuscript Received December 21, 1998

ABSTRACT: The Holliday junction is a central intermediate in genetic recombination. It contains four strands of DNA that are paired into four double helical arms that flank a branch point. In the presence of Mg^{2+}, the four arms are known to stack in pairs forming two helical domains whose orientations are antiparallel but twisted by about 60°. The basis for the antiparallel orientation of the domains could be either junction structure or the effect of electrostatic repulsion between domains. To discriminate between these two possibilities, we have constructed and characterized an analogue, called a bowtie junction, in which one strand contains a 3′,3′ linkage at the branch point, the strand opposite it contains a 5′,5′ linkage, and the other two strands contain conventional 3′,5′ linkages. Electrostatic effects are expected to lead to an antiparallel structure in this system. We have characterized the molecule in comparison with a conventional immobile branched junction by Ferguson analysis and by observing its thermal transition profile; the two molecules behave virtually identically in these assays. Hydroxyl radical autofootprinting has been used to establish that the unusual linkages occur at the branch point and that the arms stack to form the same domains as the conventional junction. Cooper−Hagerman gel mobility analyses have been used to determine the relative orientations of the helical domains. Remarkably, we find them to be closer to parallel than to antiparallel, suggesting that the preferred structure of the branch point dominates over electrostatic repulsion. We have controlled for the number of available bonds in the branch point, for gel concentration, and for the role of divalent cations. This finding suggests that control of branch point structure alone can lead to parallel domains, which are generally consistent with recombination models derived from genetic data.

The Holliday (*1*) junction is the most prominent intermediate in genetic recombination. It is known to be involved in site specific recombination (*2*−*4*), and it is likely to be involved in homologous recombination. The branch point of the Holliday junction is typically flanked by regions of dyad (homologous) sequence symmetry; this symmetry enables the molecule to undergo branch migration, an isomerization that permits the branch point to relocate. Most of our information about the physical properties of branched junctions (*5*, *6*) derives from the study of immobile DNA branched junctions (*7*); these are synthetic four-stranded complexes in which the sequence symmetry has been destroyed, thereby fixing the site of the branch point. J1, a well-characterized junction (*8*, *9*), is shown at the top of Figure 1a; its strands are numbered with Arabic numerals, and its double helical arms with Roman numerals. The accepted structural model for the immobile junction in solution is that pairs of adjacent arms stack to form two helical domains (*10*). A consequence of this conformation is that two strands have a structure similar to strands in conventional double helical DNA, whereas the other strands effect the crossover between domains; these strands are termed the "helical" and "crossover" strands, respectively. The particular stacking arrangement [(I/II and III/IV) or (II/III and IV/I)] is a function of the nucleotide pairs that flank the branch point (*11*); the stacking arrangement in J1 is I/II and III/IV (*10*). In some cases, the free energy difference between these two conformers is small enough that both species can be detected (*12*, *13*).

The relative orientation of the two helical domains is a matter of considerable interest. One of the puzzling findings of the solution analysis of immobile branched junctions is that the helical domains are most likely to be oriented in an antiparallel fashion (see the top of Figure 1b) (*14*−*16*). In addition, we have noted that the antiparallel orientation leads to greater stability for model DNA double crossover molecules, whose helix axes are confined to be coplanar (*17*). Antiparallel helix axes are not in line with models of recombinational intermediates derived from genetic experiments, because homologous nucleotides are not in proximity to each other, except near the branch point. Nevertheless, it is not difficult to see an apparent reason antiparallel helices might be preferred in solution: Model building (*18*) of branched junctions with two helical domains indicates that there is likely to be considerable electrostatic repulsion between the two domains in a parallel-like conformation but

† This research has been supported by Grants GM-29554 from the National Institute of General Medical Sciences, N00014-98-1-0093 from the Office of Naval Research, NSF-CCR-97-25021 from the National Science Foundation/DARPA, and F30602-98-C-0148 from the Information Directorate of the Air Force Research Laboratory located at Rome, NY.

* Address correspondence to this author (ned.seeman@nyu.edu).
‡ New York University.
§ University of the Sciences in Philadelphia.

10.1021/bi9823479 CCC: $18.00
Published on Web 02/11/1999

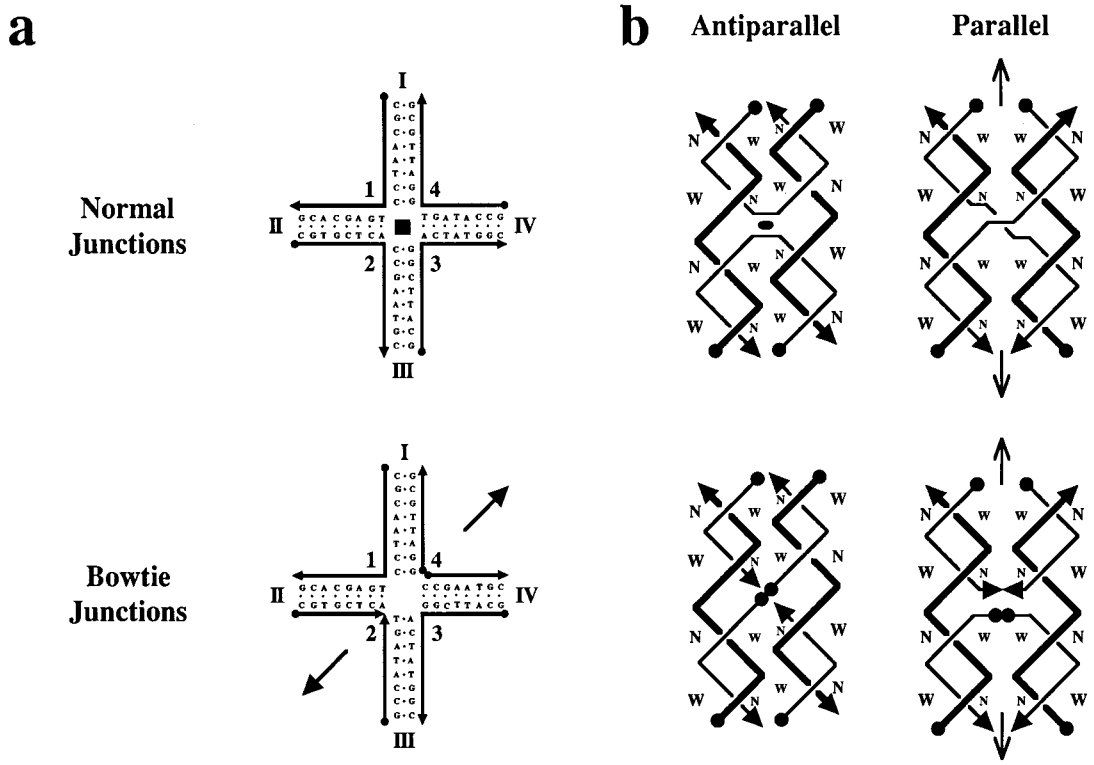

FIGURE 1: Conventional and bowtie branched junctions. (a) Schematic drawings. The upper drawing shows the well-characterized immobile branched junction, J1, composed of four conventional strands of DNA. The strands are labeled with Arabic numerals, and the double helical arms, with Roman numerals. The 5′ ends of strands are indicated by filled circles, and the 3′ ends are indicated by arrowheads. Unlike a Holliday junction, there is no 2-fold sequence symmetry at the branch point, so the position of the crossover cannot relocate through branch migration. The potential 4-fold symmetry of the backbone is indicated by the filled black square at the center of the branch point. The lower drawing shows the same junction converted to a bowtie junction. The sequences of strands 1 and 3 have been retained. Strand 2 now has two 5′ ends and a 3′,3′ linkage at the branch point; likewise, strand 4 has two 3′ ends and a 5′,5′ linkage at the branch point. The unusual linkages restrict the bowtie junction backbone to 2-fold symmetry, about the axis indicated by two arrows on the diagonal. (b) Conformations of conventional and bowtie junctions. The same conventions apply as in (a). The top panel shows the strand structures of the antiparallel (left) and parallel (right) conventional branched junction if its arms stack to form two helical domains. The helical strands [strands 1 and 3 of (a)] are drawn with a thick line, and the crossover strands [strands 2 and 4 of (a)] are drawn with a thin line. Major (wide) and minor (narrow) grooves are indicated by "W"s and "N"s, respectively, on both sides of each helical domain; the abutting surface on the inside of the molecule has smaller characters for reasons of clarity. Note that the major groove abuts a minor groove in the antiparallel junction but that minor grooves abut minor grooves and major grooves abut major grooves in the parallel junction. There is a dyad axis normal to the page in the antiparallel structure, indicated by the lens-shaped figure at its center. The dyad axis of the parallel conformation lies in the plane of the page and is indicated by the two arrowheads at the center. The bottom panel shows bowtie junctions drawn the same way. There is a dyad axis normal to the antiparallel bowtie junction at its center, but it has been omitted for clarity. The parallel bowtie junction has a branch point structure similar to the antiparallel conventional junction.

that the repulsion appears to be somewhat lower in an antiparallel-like conformation. The top of Figure 1b shows that strands abut each other in a major groove-to-major groove and minor groove-to-minor groove arrangement in a parallel conformation. In antiparallel structures, every other interdomain strand juxtaposition is longer, because they abut major groove-to-minor groove. However, this explanation is not the only one conceivable: an alternative hypothesis for the origin of antiparallel helical domains would suggest that the conformation is determined by the detailed local structure of the branch point.

One way to distinguish these hypotheses is to construct branched junctions containing unusual 5′,5′ and 3′,3′ linkages in the crossover strands. The conversion of J1 to such a junction is shown in the bottom portion of Figure 1a. In these structures, the conventional local branch point structure, in which the crossover strands reverse direction, would lead to parallel helical domains, but the opposite branch point structure would lead to the antiparallel arrangement (see Figure 1b). By contrast to conventional junctions, the usual major groove-to-minor groove domain relationship would lead to a crossover structure similar to that of the parallel conventional junction (Figure 1b). Thus, this system provides a means to establish the basis for the antiparallel structure of the immobile junction.

We have constructed branched junctions containing 5′,5′ and 3′,3′ linkages. The 3′,3′ linkage is represented by two opposing arrowheads, resembling a bowtie (Figure 1b), so we name these junctions "bowtie" junctions. We have analyzed the structure of these molecules in solution by means of Cooper−Hagerman gel mobility experiments (*19*), and we have compared them with conventional branched junctions containing identical sequences in their helical strands. Surprisingly, we find that these molecules adopt a parallel conformation, suggesting that the long-range electrostatic contribution to the orientation of the helices is less important for junction conformation than the local structure of the branch point.

MATERIALS AND METHODS

DNA Synthesis and Purification. All DNA molecules used in this study were synthesized on an Applied Biosystems

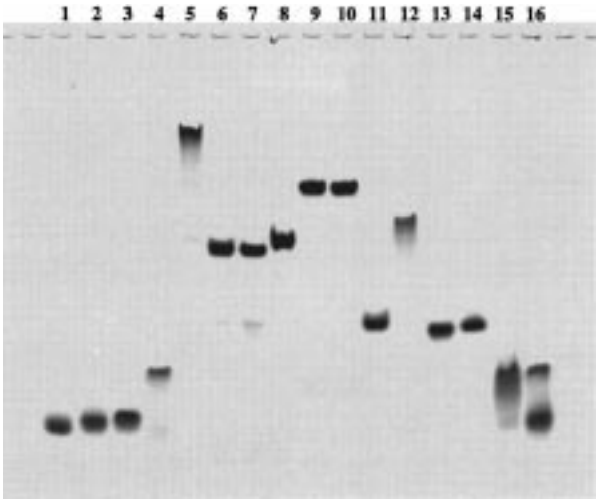

FIGURE 2: Nondenaturing gel containing stoichiometric mixtures of bowtie junction components. This is a 12% nondenaturing gel containing stoichiometric mixtures of the individual strands. Lanes 1−4 contain individual strands 1, 2, 3, and 4, respectively. Lanes 5−8 contain the triple mixtures lacking strands 4, 3, 2, and 1, respectively. Lanes 11−16 contain the pairwise combinations 1 + 2, 2 + 3, 3 + 4, 4 + 1, 1 + 3, and 2 + 4, respectively. Lane 9 contains the complete complex, 1 + 2 + 3 + 4, and lane 10 contains the normal junction of the same size as a control. Some of the subcomponent mixtures (4, 1 + 2 + 3, 2 + 3) migrate anomalously, probably due to oligomerization. However, the complete bowtie junction complex in lane 9 migrates virtually identically with the normal junction in lane 10, without breakdown or higher bands being evident.

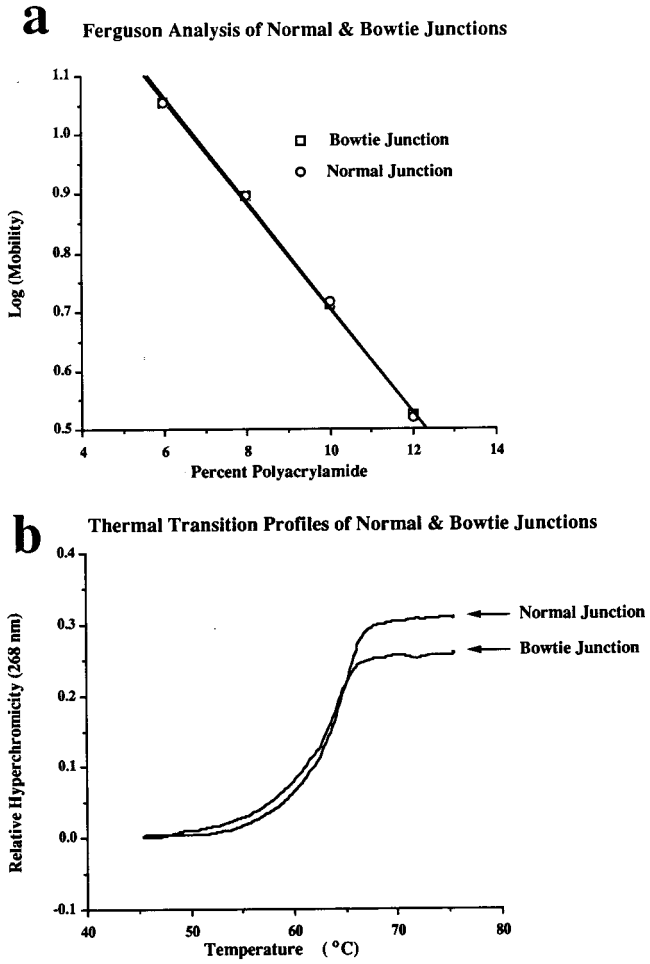

FIGURE 3: Physical characterization of the bowtie and normal junctions. (a) Ferguson plots. The logarithm of electrophoretic mobilities of the bowtie (squares) and normal (circles) junctions are plotted against the weight percent of polyacrylamide in a series of gels. The two plots are virtually superimposable. The slope of the bowtie junction is −0.083 50, and its intercept is 1.591. The slope of the normal junction is −0.089 05, and its slope is 1.597. (b) Thermal transition profiles. The melting profiles of both molecules are very similar, although more relative hyperchromicity is seen in the case of the normal junction.

380B automatic DNA synthesizer, removed from the support, and deprotected using routine phosphoramidite procedures (*20*). Strands 2 and 4 have been synthesized by substituting 5′ phosphoramidites (Glen Research) for conventional 3′ phosphoramidites in half the synthesis. Yields are not significantly reduced by switching polarities. All strands were purified by polyacrylamide gel electrophoresis. Strand 4 has been radioactively labeled at its lower-numbered end (Figure 4), where necessary, by the addition of a labeled nucleotide using the Klenow fragment of DNA polymerase to fill in a complement to a 3-nucleotide overhang; the overhang is created by pairing to strand 4 a molecule complementary to the end to be labeled. In a similar fashion, the lower-numbered end of strand 2 (Figure 4) was hybridized to a complement with an extension; a labeled hexanucleotide was ligated to the strand. Labeled strands 2 and 4 were repurified by denaturing gel electrophoresis. Large molecules used in reporter-arm mobility studies were constructed by ligating reporter arms to a central core.

Formation of Hydrogen-Bonded Complexes. Complexes are formed by mixing a stoichiometric quantity of each strand, as estimated by OD_{260}. This mixture is then heated in a buffer containing 40 mM Tris·HCl, pH 8.0, 20 mM acetic acid, 2 mM EDTA, and 12.5 mM magnesium acetate (TAEMg) to 90 °C for 5 min and cooled to the desired temperature by the following protocol: 20 min at 65 °C, 20 min at 45 °C, 30 min at 37 °C, 30 min at room temperature, and (if desired) 2 h at 4 °C. Stoichiometry is determined by titrating pairs of strands designed to hydrogen bond together and visualizing them by native gel electrophoresis; the absence of monomer indicates the endpoint.

Thermal Denaturation Profiles. DNA strands were dissolved to 1 μM concentration in 2 mL of a solution containing 40 mM sodium cacodylate and 10 mM magnesium acetate, pH 7.5, and annealed as described above. The samples were transferred to quartz cuvettes, and the cacodylate buffer was used as a blank. Thermal denaturation was monitored at 260 nm on a Spectronic Genesys 5 spectrophotometer, using a Neslab RTE-111 circulating bath; temperature was incremented at 0.1 °C/min.

Hydroxyl Radical Analysis. Individual strands of the complexes are radioactively labeled and are additionally gel purified from a 15% denaturing polyacrylamide gel. Each of the labeled strands [approximately 1 pmol in 50 mM Tris·HCl (pH 7.5) containing 10 mM $MgCl_2$] undergoes one of the following actions: annealed to a 100-fold excess of the unlabeled complementary strands; annealed to a 100-fold excess of a mixture of the other strands forming the complex; left untreated as a control; treated with sequencing reagents (*21*) for a sizing ladder. The samples are annealed as described above. Hydroxyl radical cleavage of the double-strand and junction samples for all strands takes place for 2 min (*22*), with modifications noted by Churchill et al. (*10*). The reaction is stopped by addition of thiourea and is then

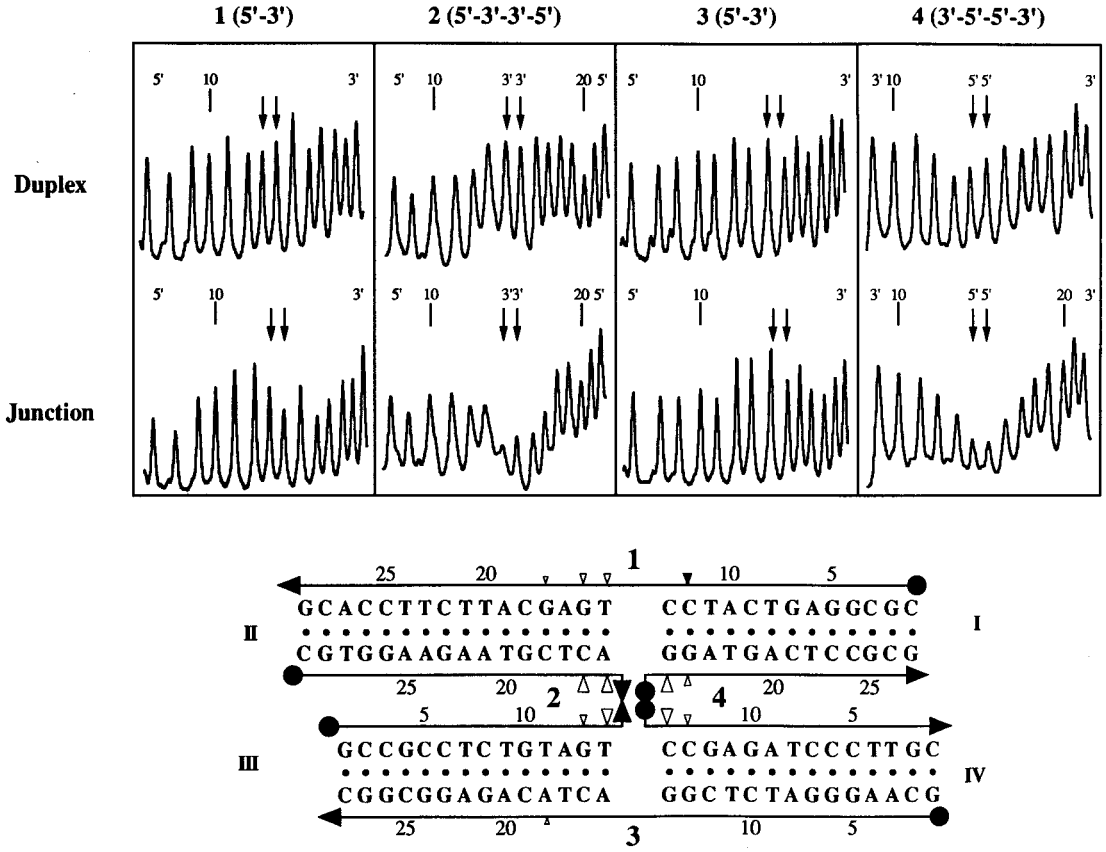

FIGURE 4: Hydroxyl radical footprinting patterns of the bowtie junction. The upper panel illustrates scans of the individual strands in the duplex (above) or in the bowtie junction (below). The 5′ ends of each strand or strand portion are indicated. The nucleotides flanking the branch point location are indicated by a pair of downward pointing arrows. There are inherent numbering ambiguities in strands 2 and 4 that are resolved in the schematic drawing of the molecule below the scans; this molecule represents the entire sequence of the bowtie junction used in this work. 3′ ends are indicated by arrowheads, and 5′ ends are indicated by filled circles. The sites of protection are indicated by the open triangles, and the extent is indicated qualitatively by their size. The unusual enhancement seen here is indicated by the small filled triangle. The gaps between arms in the two helical domains are present only to accommodate the notation. It is clear that the major sites of protection in the bowtie junction, relative to duplex DNA, are at the 3′,3′ and 5′,5′ linkages, suggesting that they are the site of the crossover between helical domains.

precipitated with ethanol. The sample is dried, dissolved in a formamide/dye mixture, and loaded directly onto a 15% polyacrylamide/8.3 M urea sequencing gel. Autoradiograms are analyzed on a BioRad GS-525 molecular imager.

Polyacrylamide Gel Electrophoresis

Denaturing Sequencing Gels. These gels contain 8.3 M urea and are run at 55 °C. The gels contain 14% acrylamide (19:1, acrylamide:bisacrylamide). The running buffer consists of 89 mM Tris·HCl, pH 8.0, 89 mM Boric acid, and 2 mM EDTA (TBE). The sample buffer consists of 10 mM NaOH and 1 mM EDTA, containing 0.1% Xylene Cyanol FF tracking dye. Gels are run on an IBI Model STS 45 electrophoresis unit at 70 W (50 V/cm), constant power, dried onto Whatman 3MM paper, and exposed to X-ray film for up to 15 h.

Nondenaturing Gels. Gels contain 4−15% acrylamide (29:1, acrylamide:bisacrylamide). DNA is suspended in 10 μL of a solution containing TAEMg; gels lacking magnesium contain only 40 mM tris, 20 mM acetic acid, and 2 mM EDTA (TAE). Samples equilibrated in TAEMg are converted to TAE conditions, when necessary, by means of a Microcon-30 spin column (Amicon, Inc.). A 1 μL volume of a solution containing TAEMg, 50% glycerol, and 0.2% each of Bromophenol Blue and Xylene Cyanol FF tracking dyes is added to the sample before loading. Gels are run on a Hoefer SE-600 gel electrophoresis unit at 8 V/cm at 4 °C and stained with Stainsall dye. Absolute mobilities (cm/h) of native gels run at room temperature are measured for Ferguson analysis; logarithms are measured to base 10.

Enzymatic Reactions

A. Kinase Labeling. A 1−13 μM amount of DNA is phosphorylated in a solution containing 66 mM Tris·HCl, pH 7.6, 6.6 mM $MgCl_2$, and 10 mM DTT and mixed with 5 μL of 2.2 μM γ-^{32}P-ATP (10 mCi/mL) and 6 units of polynucleotide kinase (U.S. Biochemical) for 2 h at 37 °C. The reaction is stopped by heat inactivation, followed by gel purification.

B. Ligations. A total of 10 units of T4 polynucleotide ligase (U.S. Biochemical) in 30 μL of a buffer supplied by the manufacturer are added to 10 pmol of each strand, and the reaction is allowed to proceed at 16 °C for 10−16 h. The reaction is stopped by heat inactivation, followed by gel purification.

C. Restriction Endonuclease Digestions. Restriction enzymes are purchased from New England Biolabs and used in the buffer (NEBuffer 2) suggested by the supplier. Junctions annealed and ligated in the ligation buffer are brought to NEBuffer 2 conditions by use of a Microcon-30

spin column. The junctions are digested for 1 h at 37 °C.

D. 3′-End Labeling of DNA. A 50 pmol amount of the strand to be labeled and its complement with a 5′ overhang is added to 5 μL of a solution containing 10× TAEMg buffer, which is then diluted to a volume of 50 μL, and the two DNA strands are then annealed as described above. To this solution are added 2 μL each of solutions containing 100 mM GTP and 100 mM CTP, 5 μL of 2.2 μM α-^{32}P-dATP (10 mCi/mL), and 5 μL (5 units/μL) of Klenow fragment (New England Biolabs). The mixture is incubated for 30 min at room temperature and is stopped by precipitation with ethanol, and the DNA molecules are purified by gel electrophoresis.

RESULTS

Sequence Design. The basis for the design of the bowtie junctions studied here is the well-characterized branched junction, J1 (8). Figure 1b shows that the four strands of a bowtie junction consist of two conventional strands (numbered 1 and 3), with a 5′ and a 3′ end, one strand with two 5′ ends (numbered 2), and one strand with two 3′ ends (numbered 4). The two conventional strands in the molecule actually used are identical to strands 1 and 3 of J1 (Figure 1a) in the vicinity of the junction. The sequences of strands 2 and 4 are determined by the selection of sequences for strands 1 and 3. A control molecule (called the normal junction) used throughout this study is a conventional branched junction in which strands 2 and 4 have been replaced with strands of DNA containing only 3′,5′ linkages. The molecule actually used (Figure 4) is somewhat longer than J1, and the other nucleotides, including those for the Cooper−Hagerman experiments, have been selected using the program SEQUIN (*23*).

Formation of the Complexes. The first issue to be addressed with a new DNA motif is whether it forms in a satisfactory fashion. We have used nondenaturing gel electrophoresis to characterize DNA branched junctions (*9*, *24*), DNA antijunctions and mesojunctions (*25*, *26*), DNA double crossover molecules (*17*), and DNA polycrossover molecules (*27*), and we have applied this method here, as well. A single band of approximately the correct molecular weight is taken as an indication that the complex has formed successfully. By contrast, bands well below the expected molecular weight indicate that the complex is unstable (*24*), and bands corresponding to multimers (*17*, *25*−*27*) suggest that the monomer contains unfavorable features. Figure 2 shows a gel containing the individual constituents of the bowtie junction used here. Lanes 1−4 contain the individual strands, lanes 11−16 contain stoichiometric mixtures of all six possible pairs of strands, and lanes 5−8 contain the four possible trimers of strands. Some of these complexes produce individual bands, and some of them produce multimers. Lane 9 contains the bowtie junction, which migrates as a single band. Lane 10 contains the best marker, the normal DNA branched junction (see Sequence Design) containing strands 1 and 3, and the appropriate 3′,5′ versions of strands 2 and 4. It runs at virtually the same mobility and also behaves as a single species on this gel. These data suggest that the bowtie junction is a tractable DNA complex.

Ferguson Analysis of Bowtie Junctions. The Ferguson plot (*28*) of log(mobility) vs percent polyacrylamide provides information about the surface of the molecule; the slope of the Ferguson plot is proportional to the friction constant of the molecule (*29*). We have compared the behavior of bowtie and normal DNA branched junctions in this form of analysis. Figure 3a illustrates the Ferguson plots of both molecules, which are virtually superimposable, indicating identical friction constants. Hence, the surface properties of the bowtie junction appear similar to those of the normal branched junction.

Thermal Transition Profiles. The melting behavior of a DNA molecule can reveal the relative stabilities of various parts of the molecule and can be used to relate the stabilities of different molecules. Figure 3b compares the melting behavior of the bowtie junction with the normal junction. Both molecules demonstrate uniphasic behavior and melt within a degree of each other; the inflection point, T_{max}, is 64.2 °C for the bowtie junction and 65.2 °C for the normal junction. Thus, the normal junction is only marginally more stable and has a higher relative hyperchromicity, possibly indicating more stacking.

Hydroxyl Radical Autofootprinting. We have used hydroxyl radical autofootprinting as a preliminary structural tool to characterize a variety of unusual DNA motifs, including branched junctions (*10*, *24*), antijunctions and mesojunctions (*25*, *26*), double crossover molecules (*17*), and polycrossover molecules (*27*). The experiment compares the quantitative hydroxyl radical cleavage pattern of each strand paired with its duplex complement to the pattern of the same strand complexed in the unusual motif. The duplex pattern serves to control for sequence effects and provides a baseline of known structure with which to compare the pattern in the unusual motif. If the cleavage pattern of the strand in the two complexes is the same, the inference is that the strand has adopted a helical structure in the unusual motif. The nucleotides flanking crossover points characteristically evince a protection from cleavage, relative to the double helical control (*10*, *24*). In the case of strand 2, containing a 3′,3′ linkage, the complementary strand used to establish the duplex pattern contains a 5′,5′ linkage opposite the 3′,3′ linkage; similarly, the duplex complement to strand 4, containing a 5′,5′ linkage, contains a 3′,3′ linkage opposite that point.

Figure 4 illustrates the results of hydroxyl radical autofootprinting analysis of the bowtie junction. The pattern for each strand in the junction is compared with its pattern in a double helix, and a qualitative picture of the protection pattern is shown on a sketch of the molecule below the scans of band intensity. There is dramatic protection relative to duplex visible at the nucleotides that flank the bowtie junction crossover points of strands 2 and 4. This feature has been seen repeatedly for the nucleotides that flank the crossover points of conventional strands; thus, strands 2 and 4 are likely to be the crossover strands of this molecule. This notion is supported by the absence of strong protection on strands 1 and 3, which are the helical strands of J1. Thus, the hydroxyl radical pattern is similar to that of J1, suggesting that the stacking of the bowtie junction is also similar to that of J1: arm I stacks on arm II and arm III stacks on arm IV to produce two stacking domains. Nevertheless, some differences with the usual J1 stacking pattern are present. The J1 junction exhibits characteristic weak protection on the helical strands (1 and 3), four nucleotides 3′ to the two

nucleotides flanking the crossover point; this protection is even weaker in the bowtie pattern and is restricted to only the nucleotide four residues 3′ to the 5′ crossover-flanking nucleotide. Weak protection is visible at the junction point of strand 1 (also noted in J1), and an unusual cleavage enhancement point is also seen 1 nucleotide 5′ to the branch point position on strand 1. Nevertheless, the conclusion drawn here is that the overall stacking arrangement is similar to that of J1 (*10*), which contains the same junction-flanking sequences in its helical strands.

Gel Mobility Studies. Although the hydroxyl radical studies confirm that the bowtie junction arranges its arms in a fashion similar to J1, this experiment does not address the relative orientation of the two domains. We have used the Cooper−Hagerman method (*19*) for determining this feature of bowtie junction structure. In this experiment, two long reporter arms are attached to the junction, in the six possible combinations available. The relative electrophoretic mobilities of these six derivatives are then assayed on nondenaturing gels. The interpretation of this experiment is predicated on the assumption that the angle between the two long reporter arms is the determining factor in the mobility of the molecule. A further assumption is that the gel retardation observed is a monotonically decreasing function of the angle between the arms: The larger the angle, the more rapidly the molecule migrates. In addition, one also assumes that the reporter arms do not perturb the structure of the junction. Conclusions based on these assumptions have been borne out in experiments involving transient electric birefringence (*30*) and fluorescence resonance energy transfer (*16*, *31*). The most rapidly migrating molecules are expected to contain reporter arms that extend a single stacking domain (if one is present); likewise, the most slowly migrating fragments are expected to reflect reporter arms that flank the smallest angles about the branchpoint of the molecule.

As a matter of convenience, we have utilized Lilley's adaptation (*14*) of the Cooper−Hagerman experiment. This entails making a single large junction (100 nucleotide pairs/arm in this work) and including unique blunt-end restriction sites on each arm; the six combinations are produced by pairwise restriction of the junction to produce a molecule in which two arms have been trimmed to 11 nucleotide pairs. Figure 5a shows the results of this experiment for the bowtie junction. Remarkably, the slowest moving fragments are those that have been restricted to leave as reporter arms I and IV or arms II and III. This pattern corresponds to a molecule whose helical strands are parallel rather than antiparallel. As expected, the most rapidly migrating molecules are those in which the individual domains established by the hydroxyl radical experiment (I/II and III/IV) contain both long arms. Likewise, the other two molecules show intermediate mobilities.

We have performed a number of control experiments to challenge this conclusion. First, we have performed the same experiment on the normal junction, containing the same reporter arms. As shown in Figure 5b, this molecule shows the usual antiparallel structure for the conventional 4-arm branched junction containing the J1 core. Again, the most rapidly migrating species contain long arms I and II or III and IV; the slowest migrating species contain reporter arms I and IV or II and III. However, now this corresponds to a junction whose helical strands are antiparallel. The constant feature in both the bowtie and normal junctions is that the crossover strands reverse direction after crossing over to the opposite domain. This point may be seen more clearly in Figure 1b. The molecules here correspond to the normal junction on the upper left or the bowtie junction on the lower right.

Five single bonds connect furanose rings in conventional 3′,5′ linkages, whereas there are four single bonds in 3′,3′ linkages and 6 single bonds in 5′,5′ linkages. We have examined the possibility that the missing bond in 3′,3′ linkages constrains the system to be parallel but that the availability of more bonds would permit it to assume the antiparallel conformation. It is straightforward to add another nucleotide, to form a deoxythymidine bulge adjacent to one of the nucleotides forming the 3′,3′ linkage. This modification adds five extra single bonds to the crossover point, not counting the extra furanose ring. Figure 5c illustrates that these extra bonds do not have a marked effect on the pattern of the bowtie junction.

An important part of the interpretation of a Cooper−Hagerman experiment is the independence of the gel mobility from the conditions of the assay. It is common for a group of unusual motifs to have Ferguson plots that intersect (*32*, *33*), so that higher mobilities on one gel may be replaced by lower mobilities on another. Indeed, this phenomenon is known to have affected the interpretation of the Cooper−Hagerman experiment (*34*). To make sure that we are not afflicted with such a problem, we have determined the Ferguson plots for each of the species in each of the gels shown in Figure 5. These are shown in Figure 6, and they establish firmly that the properties ascribed to the molecules are not a function of the 5% gels used to determine them: No reversals of mobility are seen among the components used in this analysis anywhere in the relevant range.

Another element to consider in the structure of branched junctions is the role of divalent cations. It is known that the conventional 4-arm branched junction assumes a 4-fold symmetric unstacked structure in their absence (*35*). Figure 7a demonstrates that the bowtie junction also assumes an unstacked structure; the molecules containing opposite reporter arms move most rapidly, indicating that divalent cations are involved in maintaining the stacking structure seen in their presence. Molecules containing adjacent pairs of reporter arms move in two groups of opposite sets; molecules with arms I and II or III and IV migrate more rapidly than molecules with arms I and IV or II and III. This finding suggests that the molecule differs somewhat from 4-fold symmetry; the long reporter arms linked by conventional 3′,5′ linkages appear to be have a more obtuse angle in these conditions than those with the unusual linkages. The gel mobility of the normal junction in the absence of divalent cations is shown in Figure 7b. Here, the mobilities of all four adjacent-armed molecules are almost identical.

DISCUSSION

Physical Characterization. We have demonstrated that it is possible to produce a 4-arm branched junction from a molecule containing unusual 3′,3′ and 5′,5′ linkages in two opposite strands. Under standard conditions, it forms as well as the conventional DNA branched junction. Its surface properties appear to be very similar to those of the

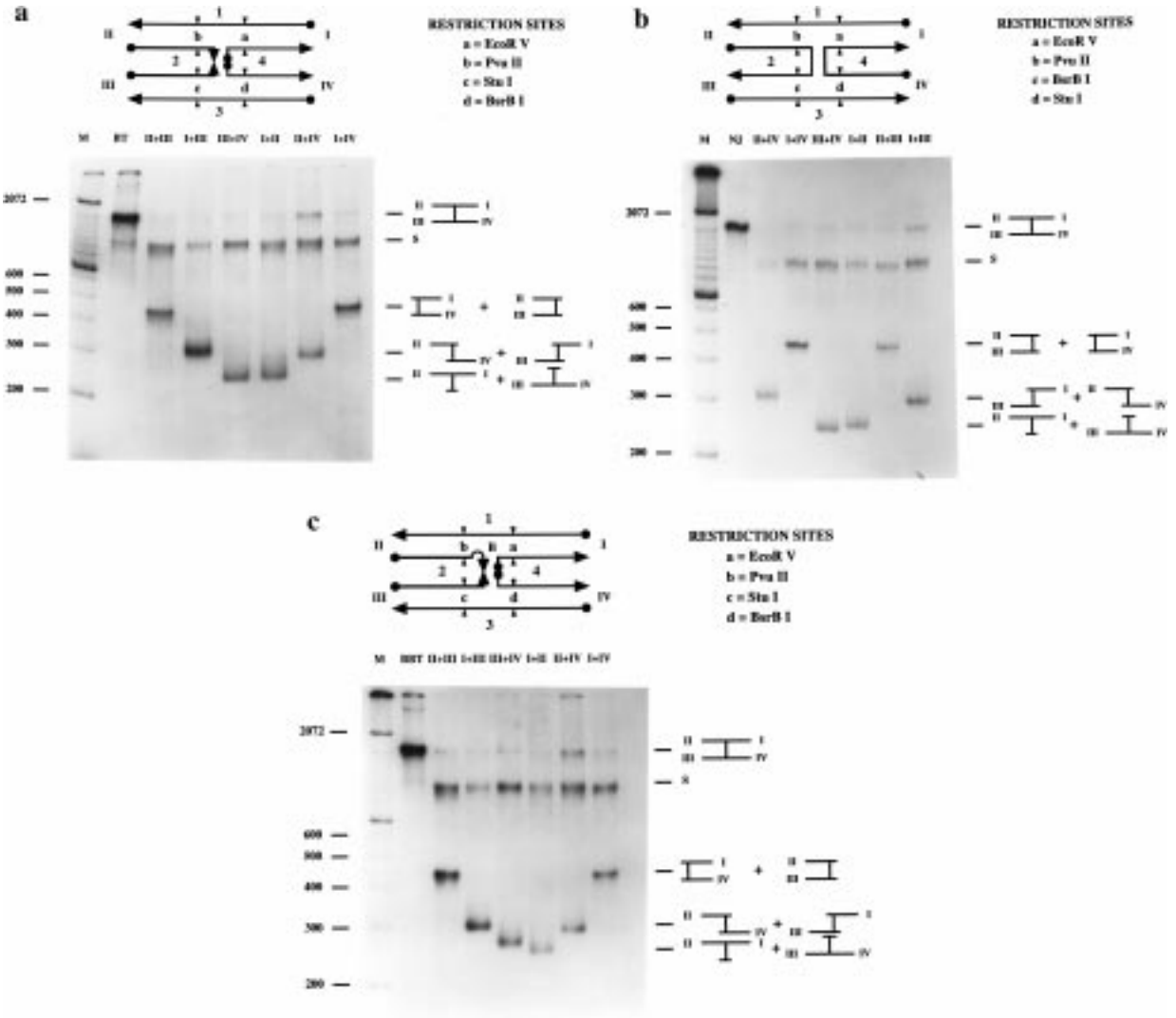

FIGURE 5: Reporter arm mobility studies of junctions. The same conventions apply to each panel. A nondenaturing 5% polyacrylamide gel is shown containing, from left to right, a series of markers, the uncleaved junction, and a series of six lanes headed by the identification of the pair of arms restricted. Above the gel is a drawing of the junction, indicating the strand numbering, the arm numbering, and the positions of cleavage in a code of a, b, c, and d. The code is explained to the right of the junction. To the right of the gel are schematic drawings of the migrating species. These drawings and the one at the top indicate the conformations derived from this experiment. It is important to realize that in all of these representations the distance between helical domains has been extended greatly so that figures can be labeled conveniently; the actual distance is only a few Ångstroms. S represents singly cleaved junctions. In all cases, the most rapidly migrating species are those restricted in arms I + II and III + IV, confirming the domain structure established by hydroxyl radical autofootprinting. (a) Bowtie junction. The slowest migrating species are those restricted in arms II + II and I + IV, indicating a parallel orientation of strands 1 and 3 and the domains to which they belong. (b) Normal junction. Note that the enzyme code differs for this panel. Again, the slowest migrating species are those restricted in arms II + III and I + IV, but now this means that strands 1 and 3 and their domains are antiparallel. (c) Bulged bowtie junction. An extra thymidine nucleotide has been included as a bulge near the junction, so as to provide more bonds in the vicinity of the 3′,3′ linkage. This is indicated by the bulge in the drawing and the "B" next to it. The pattern is similar to that in (a), from which a parallel orientation of the domains is inferred. The two species corresponding to individual domains (I + II) and (III + IV) migrate slightly differently, possibly due to the presence of the bulge, although bending of the domain containing the bulge would be expected to decrease its relative mobility, rather than increasing it.

conventional junction, and it melts within 1 °C of the normal molecule. The two conventional strands of the bowtie junction studied here are the same in the vicinity of the branch point as the helical strands of J1 (*8*); hydroxyl radical autofootprinting suggests that in the presence of divalent cations the domain structure is the same as that of J1, where strands 1 and 3 are the helical strands and strands 2 and 4 are the crossover strands. The small differences between the pattern seen with the bowtie and conventional junctions are likely to be due to domain conformational differences rather than stacking domain reversals.

We have asked whether the domain structures of the conventional and bowtie junctions are the same because of the stacking properties of those base pairs or because the bowtie linkages enforce the crossover structure. We have constructed a bowtie junction in which the 5′,5′ and 3′,3′ linkages are placed on strands 1 and 3 and strands 2 and 4 contain normal 3′,5′ linkages. When analyzed by hydroxyl radical autofootprinting, this junction is found to have the opposite crossover isomer, in which strands 1 and 3 are the crossover strands and strands 2 and 4 are the helical strands (data not shown). Thus, the presence of the bowtie junction appears to force the strands containing the 5′,5′ and 3′,3′ linkages to act as the crossover strands.

Domain Orientation. The remarkable finding here is that the orientation of the domains is opposite from that seen

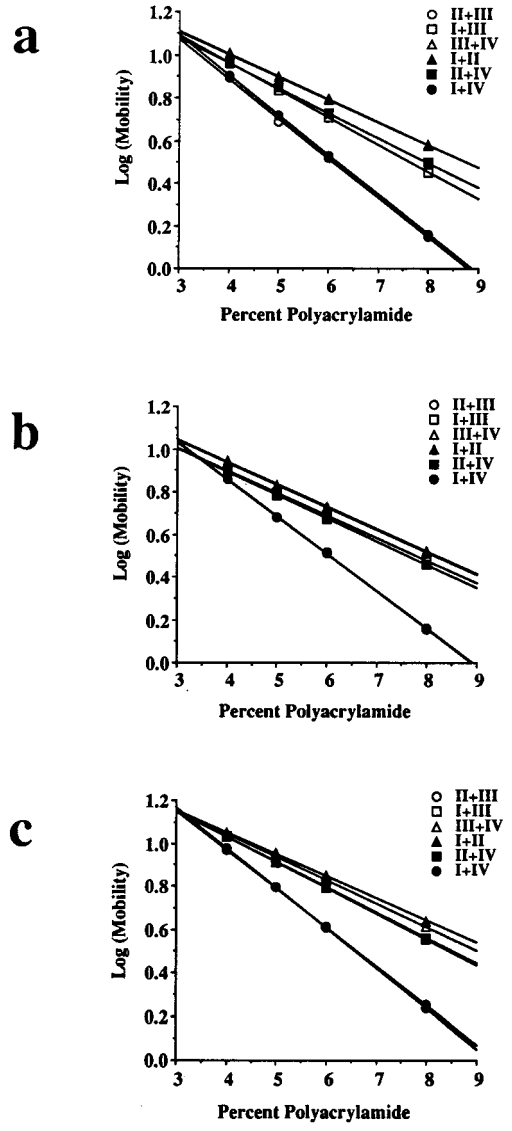

FIGURE 6: Ferguson plots of the species containing reporter arms: (a) bowtie junction; (b) normal junction; (c) bulged bowtie junction. The purpose of these plots is to ensure that the differential mobilities seen in Figure 5 are not artifacts of the gel concentration. In each panel, the complementary pairs of reporter arms are shown with symmetrical symbols, filled and empty. In each case, the most slowly migrating species, II + III and I + IV, are visibly slower at all relevant concentrations. Likewise, I + II and III + IV are the fastest at all concentrations, confirming the domain structure.

with ordinary junctions. It is clear from the mobility experiments described above that the domain orientation is parallel rather than antiparallel. There is a precedent for parallel molecules in RNA junctions (*36*), but no parallel DNA junction has been reported unless it has been constrained within a tethered (*37*), double crossover (*17*), or polycrossover (*27*) molecule. Double crossover molecules constrained to contain parallel double helical domains are often ill-behaved, forming multimers visible on nondenaturing gels (*17*); the same phenomenon has been observed with tethered junctions (*38*).

As noted above, a common explanation offered for the antiparallel structure of conventional Holliday junction analogues has been that the charge repulsion across the interdomain dyad is likely to be larger for a parallel molecule than for an antiparallel molecule (*39*). The parallel structures on the right side of Figure 1b show that the minor grooves and major grooves abut each other on either side of the dyad axis, maximizing the opportunity for electrostatic repulsion; by contrast, the antiparallel structures on the left side of Figure 1b have their grooves staggered, thereby reducing the repulsion somewhat.

The observations made here suggest that charge repulsion may be less important than the structural preferences of the branch point. The path of the backbone at the branch point of the parallel bowtie junction resembles that of the antiparallel conventional junction. As mentioned above, each of these chains changes direction as it passes through the branch point. Furthermore, the crossing pattern of the strands is the same in each case: the strands cross over each other when viewed along the vertical direction in Figure 1b (not shown) but not when viewed along the dyad axis, which is the view shown in Figure 1b. It should be noted further that the presence of the magnesium cation is a critical component of the branch point structure in solution; in its absence, neither parallel nor antiparallel helical domains are seen for either normal or bowtie junctions.

The helix axes in the conventional antiparallel Holliday analogue are not coplanar, and the domains are twisted by an angle of roughly 60° (*16*, *31*). In the parallel system, long coplanar helix axes are unlikely to be stable, because electrostatic repulsion would build up as a direct function of helix length; however, in a twisted system, the difference between parallel and antiparallel molecules would diminish as the helices extended. Thus, we expect parallel bowtie junctions to display a twisted structure, similar to antiparallel conventional branched junctions. Nevertheless, rigorously parallel DNA molecules have been noted in the analysis of oligonucleotide crystal structures, so they are not impossible in an appropriate environment (*39*).

Symmetric Immobile Junctions. We have reported previously that it is possible to create a symmetric immobile junction by coupling a symmetric junction to an immobile junction in an antiparallel double crossover molecule (*40*). These molecules have been used to analyze crossover isomerization (*12*) and branch migratory minima (*41*). Bowtie junctions can also act as symmetric immobile junctions, because the mixed strand polarities also prevent migration. They provide a system where the domain axes are able to assume a twisted and parallel-like conformation, in contrast to the coplanar antiparallel conformation of the previously reported symmetric immobile junction. The unnatural nature of the 5′,5′ and 3′,3′ linkages presents a set of artifacts different from those that accompany the use of symmetric immobile junctions derived from antiparallel double crossover molecules; thus, they can provide a useful control system for some observations made with the earlier symmetric immobile junctions (R.S., F.L., H. Iwasaki, B. Kemper, M.B., and N.C.S., in preparation).

Components of Biological Structures. The antiparallel structures determined for Holliday junction analogues have posed a major problem for combining solution physical chemistry with genetic inferences. Homologous sequences in two chromosomes are in proximity to each other in parallel molecules, but they are far apart in antiparallel molecules. It seems likely that homologous sequences should be near each other during recombination. Indeed, parallel double crossover molecules have been shown to be meiotic intermediates (*42*). Here, we have shown that it is not necessary

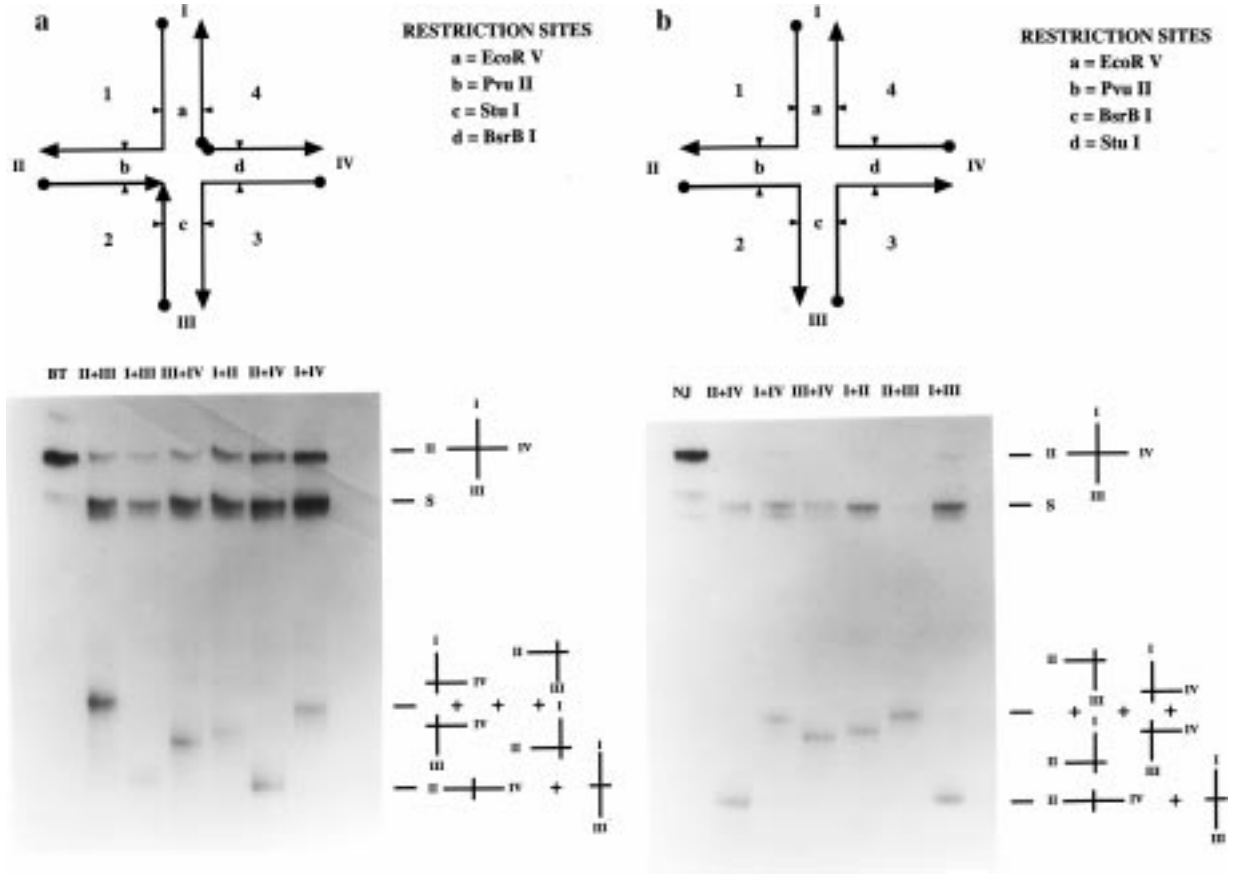

FIGURE 7: Reporter arm mobility studies in the absence of magnesium. The same conventions apply as in Figure 5. (a) Bowtie junction. The structure is dramatically different from that seen in Figure 5. The four adjacent reporter arm pairs (I + II, II + III, III + IV, IV + 1) move more slowly than the two opposite pairs (I + III, II + IV), suggesting something like the structure shown above the gel. However, the mobilities of I + IV and II + III are somewhat slower than I + II and III + IV, indicating that there are deviations from 4-fold symmetry. (b) Normal junction. The mobility pattern for the individual species is similar to that in (a), although the lanes have been loaded in a different order. This pattern is closer to a 4-fold symmetric pattern than that seen in (a) but still not ideally 4-fold symmetric.

to make major changes to the entire DNA molecule for it to assume a parallel-like structure: Only the branch point need be modified. We have performed our modification by altering the covalent structure of the molecules in a solution experiment. This is a dramatic local change to the branch point that does not appear to be available to biological systems. However, it seems possible that this sort of change could be effected by a protein molecule. The crystal structures of both Cre (*43*) and RuvA (*44*) provide precedents for proteins imposing a structure on branched junctions. It is not unreasonable to imagine that a protein could promote a parallel structure by changing the environment of the branch point in a conducive fashion.

Nanotechnological Structures. DNA nanotechnology (*45*) offers a means of controlling the structure of matter on the nanometer scale. Efforts in this direction have already produced DNA polyhedra (*46*, *47*), knots (*33*), Borromean rings (*48*), nanomechanical devices (*49*), and two-dimensional arrays with controlled surface features (*50*). The bowtie junction provides a new element that could be used in all the places that conventional junctions have been used. Branched junctions containing 3′,3′ and 5′,5′ linkages do not appear to be limited to 4-arm junctions nor to the particular arrangement used in the work described here. It remains to be seen whether they can be incorporated into double crossover molecules, the most rigid DNA motifs found to date (*51*), because their proclivity for parallel-like helical domains may ultimately destabilize them in molecules designed to contain coplanar helix axes. The other disadvantage of these molecules is the need to synthesize them chemically, because it is not possible to produce 3′,3′ or 5′,5′ linkages using DNA polymerase. Nevertheless, bowtie junctions add an element of diversity to DNA nanotechnology that may be useful in stabilizing exotic motifs and may also find applications in DNA-based computing systems (*52*) that do not entail PCR replication of molecules (e.g., ref *53*).

ACKNOWLEDGMENT

We thank Dr. David Millar for valuable discussions about junction structure.

REFERENCES

1. Holliday, R. (1964) *Genet. Res. 5*, 282−304.
2. Hoess, R., Wierzbicki, A., and Abremski, K. (1987) *Proc. Natl. Acad. Sci. U.S.A. 84*, 6840−6844.
3. Kitts, P. A., and Nash, H. A. (1987) *Nature 329*, 346−348.
4. Nunes-Duby, S. E., Matsumoto, L., and Landy, A. (1987) *Cell 50*, 779−788.
5. Lilley, D. M. J., and Clegg, R. M. (1993) *Annu. Rev. Biophys., Biomol. Struct. 22*, 299−328.
6. Seeman, N. C., and Kallenbach, N. R. (1994) *Annu. Rev. Biophys. Biomol. Struct. 23*, 53−86.
7. Seeman, N. C. (1982) *J. Theor. Biol. 99*, 237−247.
8. Seeman, N. C., and Kallenbach, N. R. (1983) *Biophys. J. 44*, 201−209.

9. Kallenbach, N. R., Ma, R.-I., and Seeman, N. C. (1983) *Nature 305*, 829−831.
10. Churchill, M. E. A., Tullius, T. D., Kallenbach, N. R., and Seeman, N. C. (1988) *Proc. Natl. Acad. Sci. U.S.A. 85*, 4653−4656.
11. Chen, J.-H., Churchill, M. E. A., Tullius, T. D., Kallenbach, N. R., and Seeman, N. C. (1988) *Biochemistry 27*, 6032−6038.
12. Zhang, S., and Seeman, N. C. (1994) *J. Mol. Biol. 238*, 658−668.
13. Miick, S. M., Fee, R. S., Millar, D. P., and Chazin, W. J. (1997) *Proc. Natl. Acad. Sci. U.S.A. 94*, 9080−9084.
14. Duckett, D. R., Murchie, A. I. H., Diekmann, S., Von Kitzing, E., Kemper, B., and Lilley, D. M. J. (1988) *Cell 55*, 79−89.
15. Lu, M., Guo, Q., Seeman, N. C., and Kallenbach, N. R. (1991) *J. Mol. Biol. 221*, 1419−1432.
16. Eis, P., and Millar, D. P. (1993) *Biochemistry 32*, 13852−13860.
17. Fu, T.-J., and Seeman, N. C. (1993) *Biochemistry 32*, 3211−3220.
18. Seeman, N. C. (1988) *J. Biomol. Struct. Dyn. 5*, 997−1004.
19. Cooper, J. P., and Hagerman, P. J. (1987) *J. Mol. Biol. 198*, 711−719.
20. Caruthers, M. H. (1985) *Science 230*, 281−285.
21. Maxam, A. M., and Gilbert, W. (1977) *Proc. Natl. Acad. Sci. U.S.A. 74*, 560−564.
22. Tullius, T. D., and Dombroski, B. (1985) *Science 230*, 679−681.
23. Seeman, N. C. (1990) *J. Biomol. Struct. Dyn. 8*, 573−581.
24. Wang, Y., Mueller, J. E., Kemper, B., and Seeman, N. C. (1991) *Biochemistry 30*, 5667−5674.
25. Du, S. M., Zhang, S., and Seeman, N. C. (1992) *Biochemistry 31*, 10955−10963.
26. Wang, H., and Seeman, N. C. (1995) *Biochemistry 34*, 920−929.
27. Shen, Z., Yan, H., and Seeman, N. C. Submitted for publication.
28. Ferguson, K. A. (1964) *Metabolism 13*, 985−1002.
29. Rodbard, D., and Chrambach, A. (1971) *Anal. Biochem. 40*, 95−134.
30. Cooper, J. P., and Hagerman, P. J. (1989) *Proc. Natl. Acad. Sci. U.S.A. 86*, 7336−7340.
31. Murchie, A. I. H., Clegg, R. M., von Kitzing, E., Duckett, D. R., Diekmann, S., and Lilley, D. M. J. (1989) *Nature 341*, 763−766.
32. Chen, J., and Seeman, N. C. (1991) *Electrophoresis 12*, 607−611.
33. Mueller, J. E., Du, S. M., and Seeman, N. C. (1991) *J. Am. Chem. Soc. 113*, 6306−6308.
34. Guo, Q., Lu, M., Churchill, M. E. A., Tullius, T. D., and Kallenbach, N. R. (1990) *Biochemistry 29*, 10927−10934.
35. Clegg, R. M., Murchie, A. I., and Lilley, D. M. J. (1994) *Biophys. J. 66*, 99−109.
36. Duckett, D. R., Murchie, A. I. H., and Lilley, D. M. J. (1995) *Cell 83*, 1027−1036.
37. Kimball, A., Guo, Q., Lu, M., Cunningham, R. P., Kallenbach, N. R., Seeman, N. C., and Tullius, T. D. (1990) *J. Biol. Chem. 265*, 6544−6547.
38. Mueller, J. E. (1991) Ph.D. Thesis, SUNY/Albany.
39. Qiu, H., Dewan, J. C., and Seeman, N. C. (1997) *J. Mol. Biol. 267*, 881−898.
40. Zhang, S., Fu, T.-J., and Seeman, N. C. (1993) *Biochemistry 32*, 8062−8067.
41. Sun, W., Mao, C., Liu, F., and Seeman, N. C. (1998) *J. Mol. Biol. 282*, 59−70.
42. Schwacha, A., and Kleckner, N. (1995) *Cell 83*, 783−791.
43. Gopaul, D. N., Guo, F., and Van Duyne, G. D. (1998) *EBMO J. 17*, 4175−4187.
44. Hargreaves, D., Rice, D. W., Sedelnikova, S. E., Artymiuk, P. J., Lloyd, R. G., and Rafferty, J. B. (1998) *Nat. Struct. Biol. 5*, 441−446.
45. Seeman, N. C. (1998) *Annu. Rev. Biophys., Biomol. Struct. 27*, 225−248.
46. Chen, J., and Seeman, N. C. (1991) *Nature 350*, 631−633.
47. Zhang, Y., and Seeman, N. C. (1994) *J. Am. Chem. Soc. 116*, 1661−1669.
48. Mao, C., Sun, W., and Seeman, N. C. (1997) *Nature 386*, 137−138.
49. Mao, C., Sun, W., Shen, Z., and Seeman, N. C. (1999) *Nature* (in press).
50. Winfree, E., Liu, F., Wenzler, L. A., and Seeman, N. C. (1998) *Nature 394*, 539−544.
51. Li, X., Yang, X., Qi, J., and Seeman, N. C. (1996) *J. Am. Chem. Soc. 118*, 6131−6140.
52. Adleman, L. M. (1994) *Science 266*, 1021−1024.
53. Winfree E. (1996) in *DNA Based Computing* (Lipton, E. J., and Baum, E. B., Eds.) pp 199−219, Am. Math. Soc., Providence, RI.

BI9823479